CHAPTER 3

Data Collection and Compilation

3.1. Water Quality Data Collection

From June 2006 to July 2011 and April 2003 to August 2011, water quality samples were taken by CSU field personnel from the Arkansas River, tributaries, and drains in the USR and DSR, respectively. During the Se study periods, 18 surface water sampling trips were made to the USR and 46 trips were made to the DSR. A total of 288 dissolved Se samples were taken and analyzed for dissolved Se and specific ions in the USR and 1,030 in the DSR during their respective study periods. Table 3.3 is a summary of the sample trips, the month and year of the trip, and the number of Se samples taken from the respective locations. Figures 3.1 and 3.2 show the dissolved Se sample locations in the USR and DSR, respectively. Tables 3.1 and 3.2 list the sample locations and their location with the river reach and segment. The location of the sample point within the segment is only listed for samples collected on the Arkansas River with respect to the location of the stream gauge within the river segment. Sample points on tributaries and drains as noted in the tables.

Sample collection trips involved hours of preparation. Before leaving for the study region(s), equipment and supplies were prepared. Peristaltic pumps were used for all surface water sample collection. Two Durham Geo TR-200 PSP peristaltic pumps were taken on each trip. The TR-200 is a single head, bi-directional, 12-volt battery operated, portable sampling pump capable of delivering flow rates up to $500\,\mathrm{mL\,min^{-1}}$ in both directions (Figure 3.3a). The pumps were cleaned, in-situ water quality instruments were calibrated, and sample collection bottles were prepared. Peristaltic pumps were cleaned at the beginning and end of each sampling day and before sampling at each field sampling location. Figure 3.4 is a picture

Table 3.1. Upstream Study Region (USR) Sample Collection Point Information. A value of zero (0) indicates the location of the segment stream gauge. Negative distances indicate the point is upstream of the reference stream gauge location. Segment B does not contain a stream gauge on the river main stem.

River Segment Name	Sample Point	Dist from USR Upstream Boundary		Dist from River Segment Stream Gauge	
		mi	km	mi	km
A	U163	0	0	-2.7	-4.3
	U161	5.8	9.3	3.1	5
	U164	6.8	10.9	4.1	6.6
B	U167	9.2	14.8		
C	U141	14.7	23.7	-5.5	-8.9
	U12	20.2	32.5	0	0
	U60	26.1	42	5.9	9.5
	U127	26.4	42.5	6.2	10
D	U74	30.3	48.8	-3.5	5.6
	U95	33.8	54.4	0	0
	U162	44	70.8	10.2	16.4
	U209	52.8	85	19	30.6
E	U207	55.1	88.7	-6.6	-10.6
	U201	61.7	99.3	0	0

Table 3.2. Downstream Study Region (DSR) Se Sample Location Information. A value of zero (0) indicates the location of the segment stream gauge. Negative distances indicate the point is upstream of the reference stream gauge location.

River Segment Name	Sample Point	Dist from USR Upstream Boundary		Dist from River Segment Stream Gauge	
		mi	km	mi	km
F	D101C	0	0	0	0
	D102C	7.9	12.7	7.9	12.7
	D23	11.6	18.7	11.6	18.7
	D103C	17.6	28.3	17.6	28.3
	D36	23.4	37.7	23.4	37.7
G	D104C	24.9	40.1	0	0
	D105C	31.2	50.2	6.3	10.1
	D57	38.1	61.3	13.2	21.2
	D106C	38.9	62.6	14	22.5

Table 3.3. Summary of USR and DSR Water Sample Events.

Trip #	Date	USR Se Samples		DSR Se Samples	
		River	Trib. & Drain	River	Trib. & Drain
1	April 2003			12	14
2	June 2003			12	15
3	July 2003			7	15
4	July 2003			6	16
5	October 2003			6	15
6	January 2004			6	15
7	March 2004			6	15
8	May 2004			6	15
9	June 2004			6	15
10	July 2004			6	15
11	August 2004			6	15
12	November 2004			6	17
13	January 2005			6	15
14	March 2005			6	15
15	June 2005			6	17
16	July 2005			6	15
17	August 2005			6	17
18	December 2005			6	16
19	January 2006			6	16
20	March 2006			6	16
21	May 2006			6	16
22	June 2006	10	5	6	16
23	July 2006			6	16
24	August 2006			6	16
25	November 2006			6	16
26	March 2007			6	16
27	May 2007	10	5	6	16
28	June 2007			6	16
29	July 2007			6	16
30	August 2007			6	16
31	October 2007	10	4		
32	November 2007			6	16
33	January 2008			6	16
34	March 2008	10	4		
35	May 2008			6	16
36	June 2008	10	5		
37	July 2008			6	16
38	August 2008	10	5		
39	November 2008			6	16
40	January 2009	10	5		

Table 3.3. Summary of USR and DSR Water Sample Events. (Continued)

Trip #	Date	USR Se Samples		DSR Se Samples	
		River	Trib. & Drain	River	Trib. & Drain
41	(No Se Samples)				
42	March 2009			6	16
43	May 2009	10	5		
44	June 2009			6	16
45	July 2009	10	4		
46	August 2009			6	16
47	November 2009	10	4		
48	January 2010			6	16
49	March 2010	10	4	6	15
50	May 2010	9	4		
51	June 2010			6	16
52	July 2010	11	6		
53	August 2010	10	7	6	17
54	November 2010	12	7	8	19
55	March 2011	12	7	8	19
56	May 2011	15	9	8	17
57	July 2011	12	7		
58	August 2011			8	17
	Totals	191	97	297	733

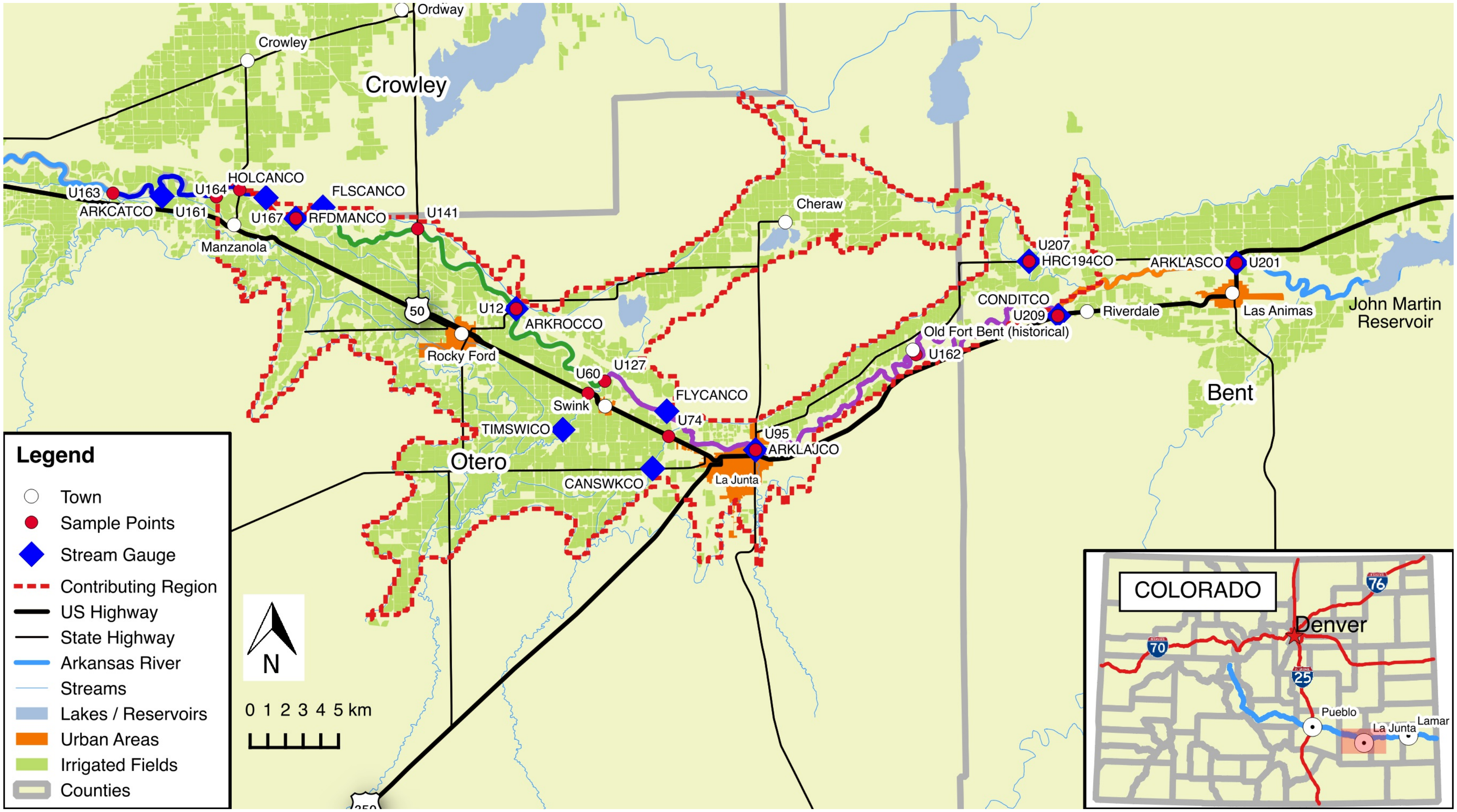

Figure 3.1. Dissolved Se sampling locations in the USR. Samples taken near, but not at stream gauge locations where shown.

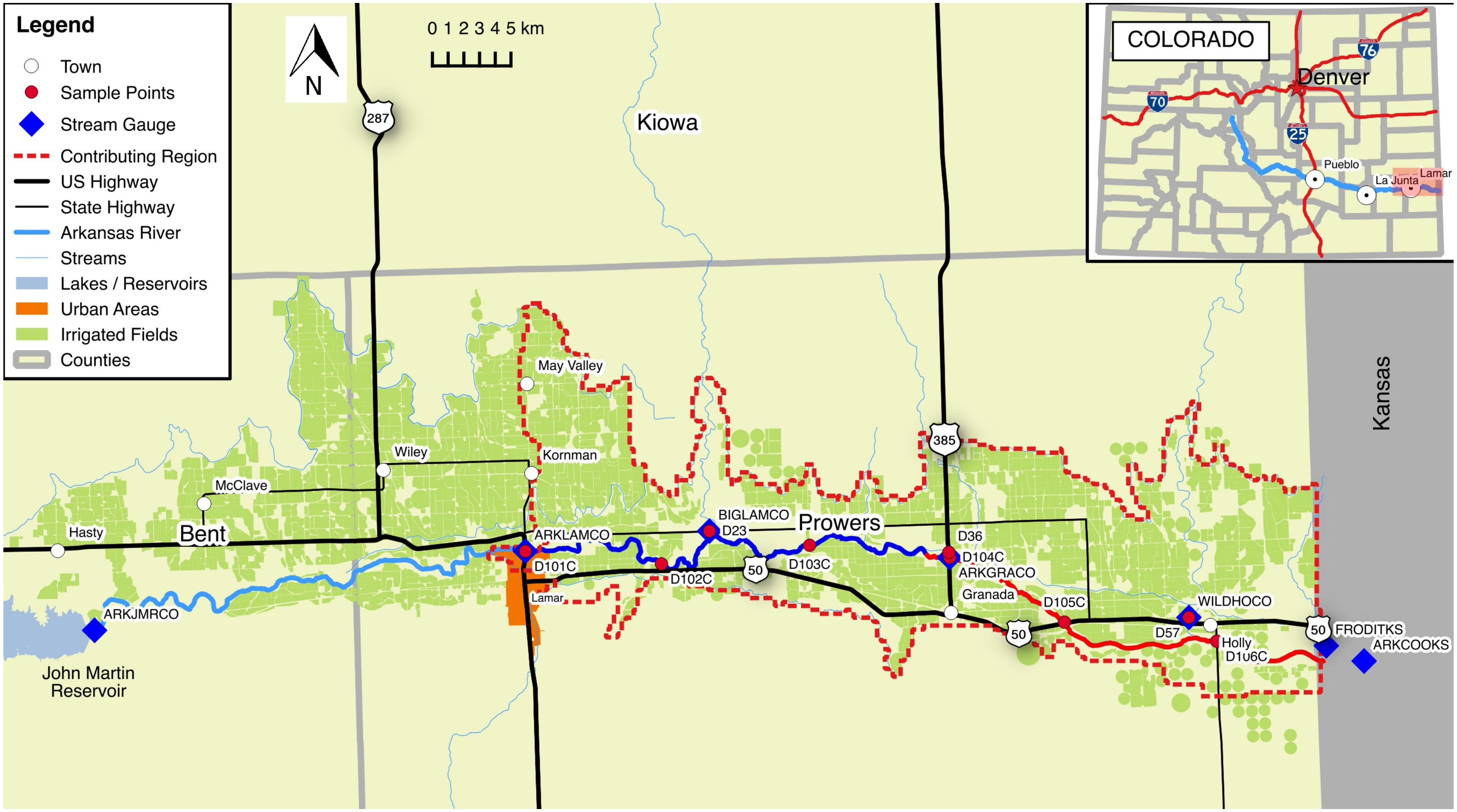

Figure 3.2. Dissolved Se sampling locations in the DSR. Samples taken near, but not at stream gauge locations where shown.

of a typical vehicle setup with cleaning buckets, peristaltic pump, water quality sonde, and various other equipment items. Cleaning consisted of the following listed procedure:

(1) At the beginning of every sampling day, four, 5-gallon (gal) buckets with lids were prepared as follows:

   (a) One bucket filled with approximately 2.5 gal tap water and approximately 20 mL of lab grade hydrochloric acid (HCl).

   (b) One bucket filled with approximately 2.5 gal tap water and approximately 20 mL of LiquiNox®, a lab grade, phosphate and ammonia free, free rinsing detergent.

   (c) Two buckets filled with approximately 2.5 gal deionized water.

(2) The acid solution was run through the pump for two minutes. This disinfected the pump tubing and prevented cross contamination.

(3) The detergent solution was run through the pump for two minutes. This removed any remaining soil particles from the pump tubing.

(4) Water from the first of the deionized water buckets was run through the pump for two minutes followed water from by the second bucket of deionized water for another two minutes. This rinsed all detergent from the pump tubing.

Two sample types were routinely taken at all locations during each trip. One sample type was for the analysis of specific ion concentrations as a general water quality panel. A 250 mL-wide mouth, high density poly-ethylene (HDPE) bottle was used to collect and ship the specific ion samples. This bottle was pre-cleaned and shipped to CSU by Ward Laboratories, Inc. in Kearney, Nebraska, the laboratory that provided the bulk of the water quality analysis services. The second sample was taken for analysis of dissolved Se concentration using a 125 mL-wide mouth, HDPE bottle. This bottle was procured from multiple sources and pre-cleaned to the US EPA's "Specifications and Guidance for Contaminant Free Sample Containers" (**EPA1992**). Approximately 0.6 mL of a diluted nitric acid solution prepared

(a) Durham Geo TR-200 PSP Peristaltic Pump.

(b) In Situ Water Quality Sonde and Data Logger. Measures temperature, specific conductivity, pH, oxidation-reduction potential, and dissolved oxygen concentration.

Figure 3.3. Water Quality Sampling Equipment.

Figure 3.4. Typical sample vehicle equipped for surface water sampling. Equipment includes peristaltic pump, water quality sonde, pump cleaning buckets, and various other equipment items. This picture is taken at sample site U162 which is on the National Park Service's Bent's Old Fort National Historic Site (fort in background).

with 33 mL of distilled water and 7 mL of ultra-pure nitric acid was added to each bottle using a graduated pipette. This was done to preserve the sample by lowering the pH to less than 2 standard pH units. During the latter half of the sampling periods, samples for dissolved uranium (U) were gathered during most sampling trips. 250 mL-narrow mouth, pre-cleaned, pre-preserved with nitric acid, HDPE bottles were provided by TestAmerica Inc., the laboratory providing dissolved uranium analysis.

Blank samples of deionized water were prepared in the lab for each sample type before each trip at the beginning of each sampling day for each sample type. Blanks are intended to be free of the analyzed constituent and are used to test the samples for bias due to contamination. Trip blanks were taken in the lab before the begining of the sample trip. They accompanied field personnel during all sampling activities and were then shipped to their respective lab for analysis. Trip blanks were intended to demonstrate that there was no contamination due to transportation activities. Field blanks were taken in the field at the begining of the sampling day. These samples also accompanied the field personnel during sampling activities and were shipped to their respective lab for analysis. Field blanks were intended to demonstrate that there was no contamination in the sampling equipment. Any variation from non-detectable solute concentration in these blanks would indicate possible contamination of the water samples taken that day and further investigation would be required. None of the lab results from field or trip blanks reported values that would indicate sample contamination.

Two YSI, Inc. 600R sondes with attached YSI, Inc. 650 MDS display data loggers were used for in-situ measurements during each sample trip (Figure 3.3b). The sondes were equipped with a Rapid Pulse polarographic dissolved oxygen (DO) sensor capable of measuring DO from $0\,\mathrm{mg\,L^{-1}}$ to $50\,\mathrm{mg\,L^{-1}}$, $\pm 2\,\%$; a thermistor capable of measuring temperature from $-5\,°\mathrm{C}$ to $50\,°\mathrm{C}$, $\pm 0.15\,°\mathrm{C}$; a glass combination electrode pH sensor capable of measuring pH in the range of 0 to 14 units, ± 0.2 units; a platinum button oxidation-reduction potential (ORP) sensor capable of measuring in the range of $-999\,\mathrm{mV}$ to $999\,\mathrm{mV}$, $\pm 20\,\mathrm{mV}$; and a four electrode, autoranging cell capable of measuring electrical conductivity (EC) as specific conductance at 25 °C in the range of 0 μS cm^{-1} to 100 000 μS cm^{-1}, ±0.5% + 1 μS cm^{-1}. The equipment was serviced and calibrated by CSU field personnel before every trip to the study reaches and at the end of every sampling day. Sondes were sent to Geotech Environmental Equipment, Inc. annually for maintenance checks. Geotech Environmental Equipment, Inc. is an authorized dealer and service provider for YSI equipment with an office in Denver, Colorado.

At least one set of duplicate water samples was taken per sampling trip to the USR and/or DSR. Duplicate, or replicate, samples were marked as 'A' and 'B' samples. The 'A' sample results were kept with the main data set and were used as the primary data set. 'B' sample results were kept separate and were used to determine the combined sampling methodology and lab analysis uncertainty. The sampling standard procedure was to take one duplicate set of surface water samples per day with a minimum of two duplicate surface water samples per sampling trip.

Each sampling event began with recording the site data on a form (log) similar to the one in Figure 3.5. In-situ water quality measurements were then taken using the YSI sonde. The data logger was used to read the data, but was not used as a recording device. All data were recorded on the form shown as an example in Figure 3.5. The ranges at the bottom of the form are maximum acceptable ranges of values determined from previous sampling trips. Values outside of these ranges would indicate to field personnel that the equipment was damaged, had lost calibration, or operational error had occured. The YSI sonde was allowed to rest in the water for a minimum of three minutes before recording values. Usually, the sonde would rest in the water while water quality samples were taken. Samples were pumped through a disposable, in-line 0.45 micron, polyethersulfone filter into the sample bottles. Peristaltic pumps were used to extract all water samples from surface water sources. No air space was permitted in any of the sample bottles. Figure 3.6a shows a trained sample collector at location U12 in the USR which is north of Rocky Ford on a bridge over the Arkansas River. The YSI sonde is not in this image, but is suspended in the river during sample collection. Figure 3.6b is the same sample collector at sample location U73 in the USR recording readings from the YSI sonde. Samples were stored on ice or in a refrigerator until they were shipped to their respective labs. Data was recorded onto the data form from the YSI sonde immediately after collectiing the water samples. The sonde was left in the water for an additional two to three minutes. Any changes in readings were recorded as a second entry. An example of a completed log is shown in Figure 3.7

Specific ion lab results from Ward Laboratories and dissolved U lab results from TestAmerica were not used directly in the analysis reported in this tesis. The Oscar E. Olson Biochemistry Laboratories (Olson Labs) at South Dakota State University (SDSU) performed dissolved Se analysis using Official Methods of Analysis of AOAC International, 17th Edition, test number 996.16, Selenium in Feeds and Premixes. This test, a fluorometric test initially designed for testing animal feeds, provides repeatable analysis for dissolved Se near criteria levels. Double tests were completed on each sample and the average was reported. The minimum reportable value was $0.4\,\mu g\,L^{-1}$.

Late in 2011, the Olson Labs was closed by SDSU for funding reasons. Staff at Olson Labs assisted CSU staff in finding a new lab capable of continuing analyses using the same methods and to the same level of quality. South Dakota Agricultural Laboratories (SDAL) was chosen. Most of the staff and equipment from Olson Labs were employed at the new SDAL providing CSU staff with ample reason to move all dissolved Se analyses to the new lab. Both Olson Labs and SDAL were certified by the USEPA for drinking water

Colorado State University
Department of Civil Engineering
Arkansas River Assessment

Surface Water Sampling Log

Station No.:				Date:
Location:				Time:
	Left	Center	Right	Sample collector(s):
Upstream				Pumping Note:
Downstream				
Location Note:				

☐ Dry ☐ Stagnant/Frozen

☐ No Access ______________________________

Time (min)	**Temp** (°C)	**Conductivity** (µS/cm)	**DO** (mg/L)	**pH**	**ORP** (mv)
Range	**(0-35)**	**(400-8000)**	**(0-18)**	**(4.8-10)**	**(-250-400)**

Figure 3.5. Example water quality sample form.

and subscribed to the proficiency testing and check sample programs for the USEPA for wastewaters . ref. How?

The same procedures and techniques for sample gathering and analysis were used during the entire sampling periods. Newer or different techniques or procedures were considered, but was determined to have the possibility to compromise the consistency of the gathered data. Results from all lab analyses were recorded in a master database at CSU for later data extraction and analysis. The data includes results from over 4,500 sample sets. Approximately 95 and 1,035 of these sample sets were taken from surface water sites in the USR and DSR, respectively. Each sample set included in-situ measurements, a dissolved

(a) Sample location U12. The Se sample bottle is being filled with a peristaltic pump through a 0.45 micron filter. The specific ion sample bottle is filled, laying next to the pump.

(b) Sample location U73. Personnel is hand logging data from the YSI sonde.

Figure 3.6. Personnel performing water sample collection.

Se sample, a general specific ion panel, and a possible dissolved U sample. In-situ EC and temperature measurements taken at stream gauge sites with permanent water quality instrumentation were compared with the measured values reported at those sites. These sites record and report EC and water temperature measurements every 15-minutes. Minor deviations were expected due to instrument drift and calibration error, yet EC and temperature differences were found to be less than 1% for all in-situ measurements.

The water and mass balance models included in this study are among the many lines of research that have used this data. Because of the multiple uses of large data sets, great care has been taken to ensure that data entry errors are rare. Data were copied into the

Colorado State University
Department of Civil Engineering
Arkansas River Assessment

Surface Water Sampling Log

Station No.:	[U201]			Date: 16 May 10
Location:	Arkansas River			Time: 1302
	Left	Center	Right	Sample collector(s): KHM
Upstream				Pumping Note:
Downstream		X		
Location Note:				

☐ Dry ☐ Stagnant/Frozen

☐ No Access ____________________

Time (min)	Temp (°C)	Conductivity (µS/cm)	DO (mg/L)	pH	ORP (mv)
4	19.40	1676	7.92	8.08	67.4

Figure 3.7. Example completed water quality sample form.

database and randomly checked for transcription errors. Original lab reports were retained on file.

3.2. River Cross-Section Geometry Survey

The Arkansas River was surveyed at twenty-one and thirteen locations in the USR and DSR, respectively. At these locations, cross-sections were surveyed and the data analyzed to determine the spatial distribution of the river geometry. The cross-sections are not equally spaced along the river segments. Cross-sections were surveyed at the extreme upstream and downstream end of each river segment. Intermediate cross-sections were located where both the landowner permitted access and the river was reasonably accessible. Additionally, the intermediate cross-sections were located where different cross-section profiles existed. This was done to capture a broadest possible range of cross-section profiles, thereby allowing for a more realistic characterization of the river geometry. Figures 3.9 and 3.10 show the locations of the surveyed cross-sections in the USR and DSR, respectively. Tables 3.4 and 3.5 describe the location of the survey point with respect to the river reach and segment. Survey locations within a river segment are with respect to the segment stream gauge location.

Industry standard survey techniques were used whenever possible. It was not possible to properly locate the instrument location in either the horizontal and vertical plane with respect to a local datum due to the remote location and the lack of available time. All data was collected with a total station (Figure 3.8a)and hand recorded into survey log books. Two back-sights were used at every surveyed cross-section. Both back-sights and the instrument location were located by using a hand held global positioning satellite (GPS) receiver (Figure 3.8b). The receiver was capable of determining the horizontal location to within ± 1 m and the vertical location to within ± 2 m. Licensed surveyors were not hired, retained, or consulted for this study.

Higher location and orientation accuracy could have been obtained by using survey grade GPS equipment or by referencing the instrument survey to an established benchmark.

Table 3.4. Upstream Study Region (USR) Survey Point Information. A value of zero (0) indicates the location of the segment stream gauge. Negative distances indicate the point is upstream of the reference stream gauge location. Segment B does not contain a stream gauge on the river main stem.

River Segment Name	Survey Point	Dist from USR Upstream Boundary		Dist from River Segment Stream Gauge	
		mi	km	mi	km
A	USS1	0	0	-2.7	-4.3
	USS2	2.7	4.3	0	0
	USS3	5.8	9.3	3.1	5
	USS4	7.8	12.6	5.1	8.2
B	USS6	9.2	14.8		
	USS7	9.3	14.9		
	USS8	10.2	16.4		
C	USS10	13.4	21.6	-6.8	-10.9
	USS11	18.1	29.1	-2.1	-3.4
	USS12	20.2	32.5	0	0
	USS13	24.4	39.3	4.2	6.8
	USS14	29.3	47.2	9.1	14.6
D	USS16	30	48.3	-3.8	-6.1
	USS17	32.6	52.5	-1.2	-1.9
	USS18	33.8	54.4	0	0
	USS19	35.9	57.8	2.1	3.4
	USS21	44	70.8	10.2	16.4
	USS22	46.4	74.7	12.6	20.3
	USS23	50.3	81	16.5	26.6
E	USS26	55.7	89.6	-6	-9.7
	USS27	61.7	99.3	0	0

For almost all surveyed cross-sections, benchmarks were not located within a reasonable distance. Attempting to tie into these benchmarks would results in an order of magnitue or more increase in the time required to complete the survey. There were also doubts as to whether the horizontal and vertical accuracy could be maintained due to the distance between the nearest benchmarks and the survey sites and the surveyor's skill. Survey grade GPS equipment could have been used, but would have required either a larger team or a significantly increased risk of equipment tampering or theft. The available survey grade

Table 3.5. Downstream Study Region (DSR) River Cross-Section Survey Location Information. A value of zero (0) indicates the location of the segment stream gauge. Negative distances indicate the point is upstream of the reference stream gauge location.

River Segment Name	Survey Point	Dist from USR Upstream Boundary		Dist from River Segment Stream Gauge	
		mi	km	mi	km
F	DSS1	0	0	0	0
	DSS4	7.9	12.7	7.9	12.7
	DSS5	10.3	16.6	10.3	16.6
	DSS6	14.9	24	14.9	24
	DSS7	17.6	28.3	17.6	28.3
	DSS8	20.5	33	20.5	33
	DSS9	23.4	37.7	23.4	37.7
G	DSS10	23.5	37.8	-1.4	-2.3
	DSS13	29.3	47.2	4.4	7.1
	DSS14	31.2	50.2	6.3	10.1
	DSS15	33.9	54.6	9	14.5
	DSS16	37	59.5	12.1	19.5
	DSS17	38.9	62.6	14	22.5
	DSS20	46.2	74.4		

(a) Pentax PCS-315 Total Station.

(b) TopCon GMS-2 Sub-meter handheld GPS.

Figure 3.8. Survey Equipment.

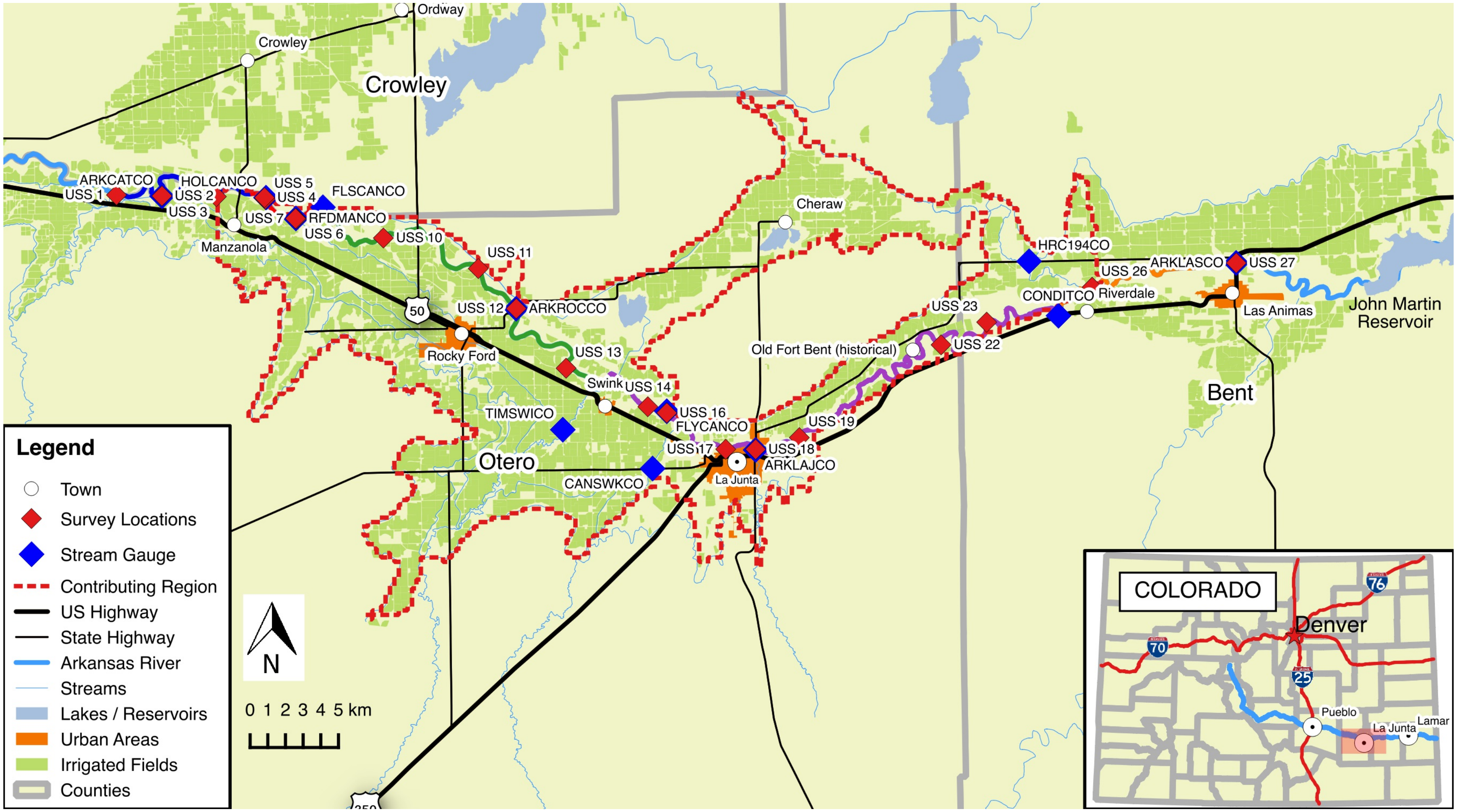

Figure 3.9. USR River Cross-section Survey Locations. Cross-sections are taken above and/or below the diversion structure and near gauge locations.

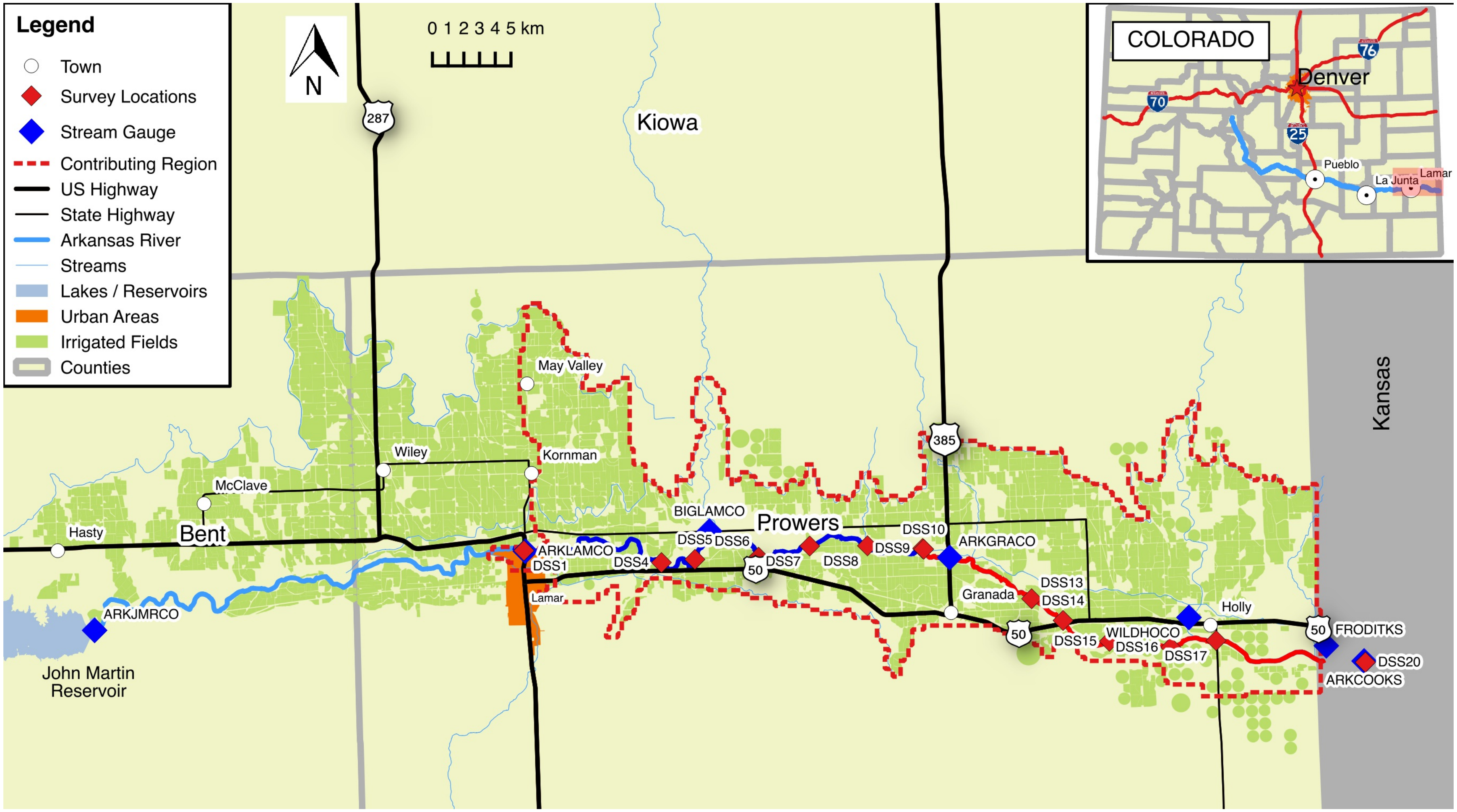

Figure 3.10. DSR River Cross-section Survey Locations. Cross-sections are taken above and/or below the diversion structure and near gauge locations.

GPS base station also had a limited range compared to the range required to access many of the locations. Since the goal of the survey was to determine the relationship between the depth and width of the river, it was determined that locating and orienting the survey data correctly was a secondary goal. For these reasons, it was determined that the level of location and orientation accuracy obtained by using the hand held GPS receiver would be sufficient.

The data was collected in the form of horizontal angle, vertical angle, sight distance, rod height, and instrument height. The survey data was downloaded from the total station and entered into a spreadsheet for conversion to horizontal and vertical location relative to the instrument. Values in the spreadsheet were checked against the survey log book. Points collected but not used to calculate the cross-section, such as the back-sight points, were marked so that they were not used in the cross-section analysis. These excluded points were used for other survey related calculations. The rod height for each measurement and the instrument height for the survey was transferred from the log book to the spreadsheet.

Coordinate geometry (COGO) techniques were used to convert from angle, sight distance, rod height, and instrument height measurements to horizontal and vertical distance measurements relative to the instrument as shown in figure 3.11. Vertical angles were measured using decimal degrees such that zero degrees ($0°$) was located above the instrument and $90°$ was horizontal. Horizontal angles were measured using decimal degrees such that $0°$ was located when the instrument was facing the first back-sight and positive angles were measured clockwise when viewed from above. The sight distance was measured using the instruments integrated laser distance measuring tool from the optics of the instrument to the rod prism with sub-millimeter accuracy. Horizontal and vertical distances to the ground location of the survey point from the ground location of the instrument were calculated as shown in equations 1 and 2, respectively. The horizontal location was calculated as northing and easting with the line between the instrument and the first back-sight as the reference. Northing and easting distances were calculated with respect to the horizontal line between the instrument and the first backsight. Corrections were made to orient the points to the coordinate system, but this step was not necessary to provide the necessary results.

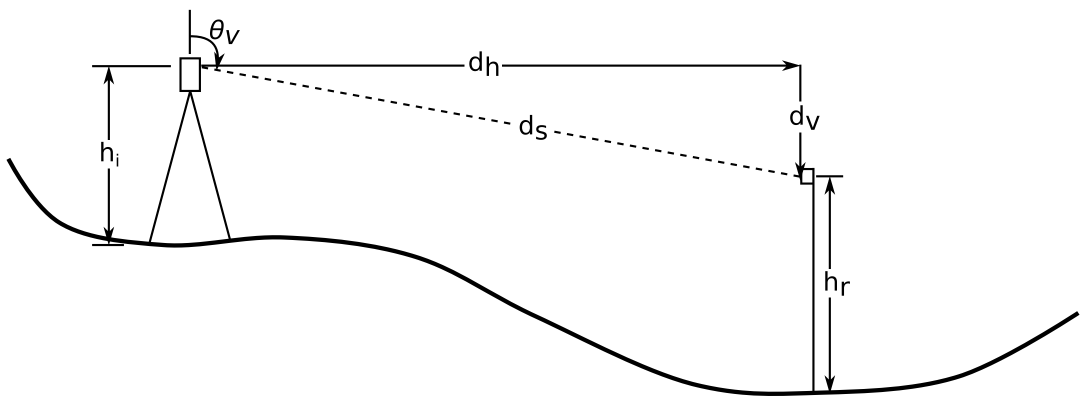

$$d_h = d_s \cdot sin(\theta_v) \tag{1}$$

$$d_v = h_i - h_r + d_s \cdot cos(\theta_v) \tag{2}$$

$d_h =$ Horizontal distance from the instrument to the surveyed point.
$d_v =$ Vertical distance from the instrument to the surveyed point.
$d_s =$ Sight distance from the instrument optics to the rod prism.
$\theta_v =$ Vertical angle from the sight optics to the rod prism

Figure 3.11. Survey Measurement Definitions.

GPS location data for the instrument and back-sights was collected in the form of northing, easting, and elevation. Colorado State Plane-South, North American Datum 1983 (NAD83), U.S. feet was used as the horizontal datum and North American Vertical Datum 1988 (NAVD88) was used as the vertical datum. All survey units are U.S. Feet. Survey errors, also known as closing errors, were corrected for all points. Most survey locations were on soft soils. It was assumed that survey error would primarily consist of instrument location drift. Measurements were taken to both back-sights at the beginning an end of the site survey. The northing, easting, and elevation difference between the measurements taken at the beginning and end of the site survey were spread equally and successively among all points. Since two back-sights were used, the total closing error was taken as the average of the closing errors for the two back-sights.

Correction of closing errors was required to obtain accurate stream depth and river top width values. Location and orientation error correction was not required and was only performed as a manner of good survey practice. Survey data points were translated from their position relative to the instrument to their position relative to the State Plane coordinate system by adding the northing, easting, and elevation values collected by the GPS receiver at the instrument site. Orientation error corrections to make instrument North coincide with true North were made by adding a positive horizontal correction angle such that the corrected angle to the first back-sight, which was the zero back-sight, matched the angle between the two corresponding GPS northing and easting coordinate sets. Final survey locations should always have the most correct location and elevation relative to a given datum. Both the back-sights and instrument location were marked with steel reinforcement bar (re-bar) and plastic caps (Figure 3.12), it may be possible for future surveys to be conducted at the same locations with the same back-sights.

Figure 3.12. Typical plastic cap on rebar used to locate instrument location and back-sights.

A least squares fit linear regression equation was fit to the relative location of all points along the surveyed cross-section (Figure 3.13). It was reasoned that a straight line through the data points would allow for a better approximation of the river's cross-section than connecting the points. The straight line would represent a true cross-section, whereas connecting the points would exaggerate the distance across the cross-section. The relative locations of the points as projected onto the best-fit line were entered into computer aided design and drafting (CADD) software (Figure 3.14). Horizontal lines, spaced 0.03 m (0.1 ft) apart from the bottom of the channel to 1.5 m (5 ft) from the bottom, were drawn from edge of bank to edge of bank. The vertical location of these lines was taken as the flow depth and the length of the line was taken as the river top width.

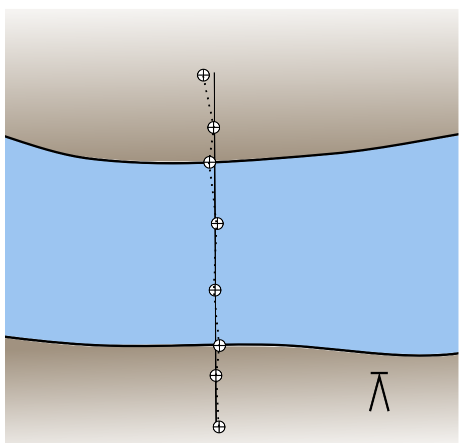

Figure 3.13. Depiction of the conversion of River Survey Locations to Linear Cross-Section. The crossed circles are the surveyed points. The instrument (total station) is in the lower right-hand corner. The dotted line depicts the cross section if no correction were made to linearize the survey cross section locations. The solid line is the cross-section line created from the best-fit line through the surveyed points. Surveyed points were translated perpendicular to the cross-section line to lie on the cross-section line across the river.

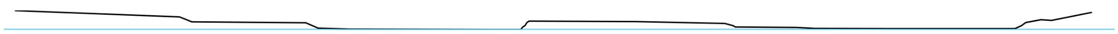

Figure 3.14. River Cross-Section as Draw in CADD Software. The black line is the channel cross-section with the left side representing the north bank of the Arkansas River (water flow is into the page). The blue horizontal line is the lowest point in the surveyed channel. All elevations were shifted such that the bottom point had a stream depth of zero. This particular cross section is at cross-section USS1. The horizontal and vertical scales are identical.

The data collected in the field constituted a small portion of the total data required to perform water and mass balance calculations. Additional data were obtained from three sources: the USGS, the CDWR, and the Colorado Climate Center (CCC).

The USGS operates and maintains the largest network of stream gauges in the United States. USGS gauges in the LARV in Colorado are operated and maintained by the USGS Colorado Water Science Center. Their main office is Lakewood, Colorado, with one of their satellite offices in Pueblo, Colorado. Of the gauges listed in Tables 3.6 and **??** and shown in Figures 3.16 and 3.17, five are operated by the USGS. There is additional sensing equipment owned and maintained by the USGS at some stream gauges owned and operated by the CDWR. Water temperature, air temperature, precipitation, and EC are the additional parameters typically measured and recorded by this equipment. EC is reported as specific conductance standardized to 25 °C and is the standard for EC used throughout this thesis. EC values are reported in units of micro-siemens per centimeter ($\mu S\,cm^{-1}$) and are converted to units of deci-siemens per meter ($dS\,m^{-1}$).

The USGS and CDWR do not have typical gauge sites in the LARV. Gauge housing and locations vary as show in Figure 3.15. These figures are not all inclusive and other variations occur in the LARV. Both agencies were consistent in the flow measuring equipment deployed to the gauge sites. During the Se sampling time frame, all stream gauges were constant flow bubblers as described in the USGS Techniques of Water Resources Investigations (TWRI) Report, Book 3, Section A, Chapter 7 (**USGS2010TWRI**). After all Se sampling was completed, the USGS and CDWR began upgrading some of the gauge sites with radar non-contact water level sensors. It is unknown how this will affect the comparison of the results of this thesis with any future work.

Table 3.6. Upstream Study Region (USR) Stream Gauge Information. Segment stream gauges record flow depth for surface area and river volume change calculations. A value of zero (0) indicates the location of the segment stream gauge. Negative distances indicate the point is upstream of the reference stream gauge location. Segment B does not contain a stream gauge on the river main stem.

River Segment Name	CDWR Stream Gauge Name	USGS Stream Gauge Name	Dist. from USR Upstream Boundary		Dist. from River Segment Stream Gauge	
			mi	km	mi	km
A	ARKCATCO		2.7	4.3	0	0
	HOLCANCO		7.8	12.6	5.1	8.2
B	RFDMANCO		9.2	14.8		
	FLSCANCO		10.2	16.4		
C	RFDRETCO		11.7	18.8	-8.5	-13.7
	ARKROCCO		20.2	32.5	0	0
	TIMSWICO	7121500	26.1	42	5.9	9.5
	FLYCANCO		29.3	47.2	9.1	14.6
D	CANSWKCO		30.3	18.8	-3.5	-5.6
	ARKLAJCO		33.8	54.4	0	0
	CONDITCO		52.8	85	19	30.6
E	HRC194CO		55.1	88.7	-6.6	-10.6
	ARKLASCO	7124000	61.7	99.3	0	0

Table 3.7. Downstream Study Region (DSR) Stream Gauge Information. River segment stream gauges record flow depth for surface area and river volume change calculations. A value of zero (0) indicates the location of the segment stream gauge. Negative distances indicate the point is upstream of the reference stream gauge location. Stream gauges ARKJMRCO, FRODITKS and ARKCOOKS although required for analysis, are not within the DSR.

River Segment Name	CDWR Stream Gauge Name	USGS Stream Gauge Name	Dist. from DSR Upstream Boundary		Dist. from River Segment Stream Gauge	
			mi	km	mi	km
	ARKJMRCO	07130500	-22	-35.4		
F	ARKLAMCO	07133000	0	0	0	0
	BIGLAMCO	07134100	11.6	18.7	11.6	18.7
	BUFDITCO		23.4	37.7	23.4	37.7
G	ARKGRACO	07134180	24.9	40.1	0	0
	WILDHOCO	07134990	38.1	61.3	13.2	21.2
	FRODITKS	07137000	43.5	70		
	ARKCOOKS	07137500	43.2	74.4		

(a) HRC194CO.

(b) BIGLAMCO.

(c) TIMSWICO

(d) FRODITKS

(e) ARKCOOKS

Figure 3.15. Range of Stream Gauge Equipment Housings in the LARV.

Data from the CDWR and USGS stream gauges are reported on web sites operated by the two agencies. Table 3.8 lists the gauge sites used in this study and notes the additional data besides streamflow collected at each gauge. Additional data are reported by the agency that owns and operates the gauge site. USGS instruments at a CDWR gauge site are recorded

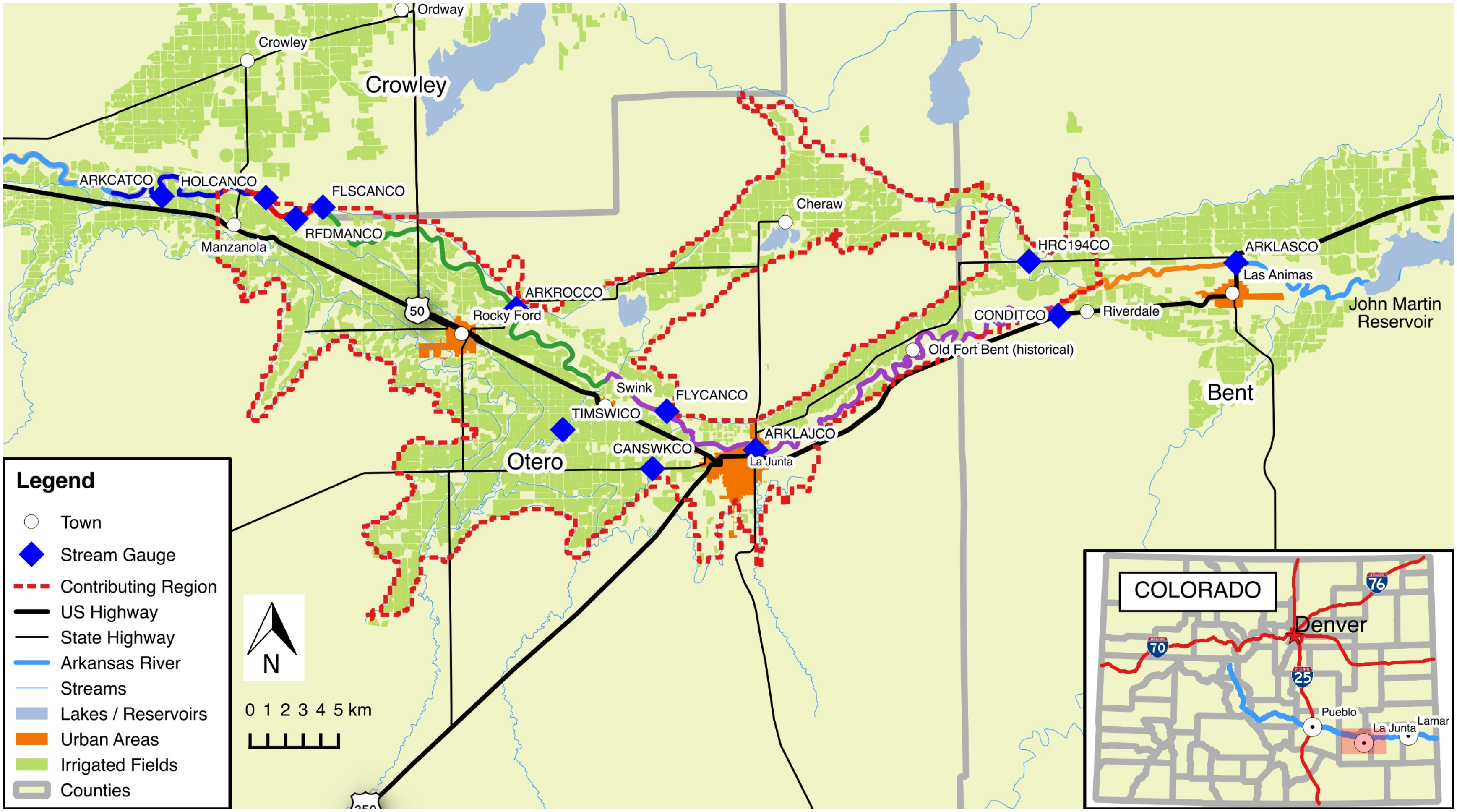

Figure 3.16. USR River River and Tributary Stream Gauge Locations.

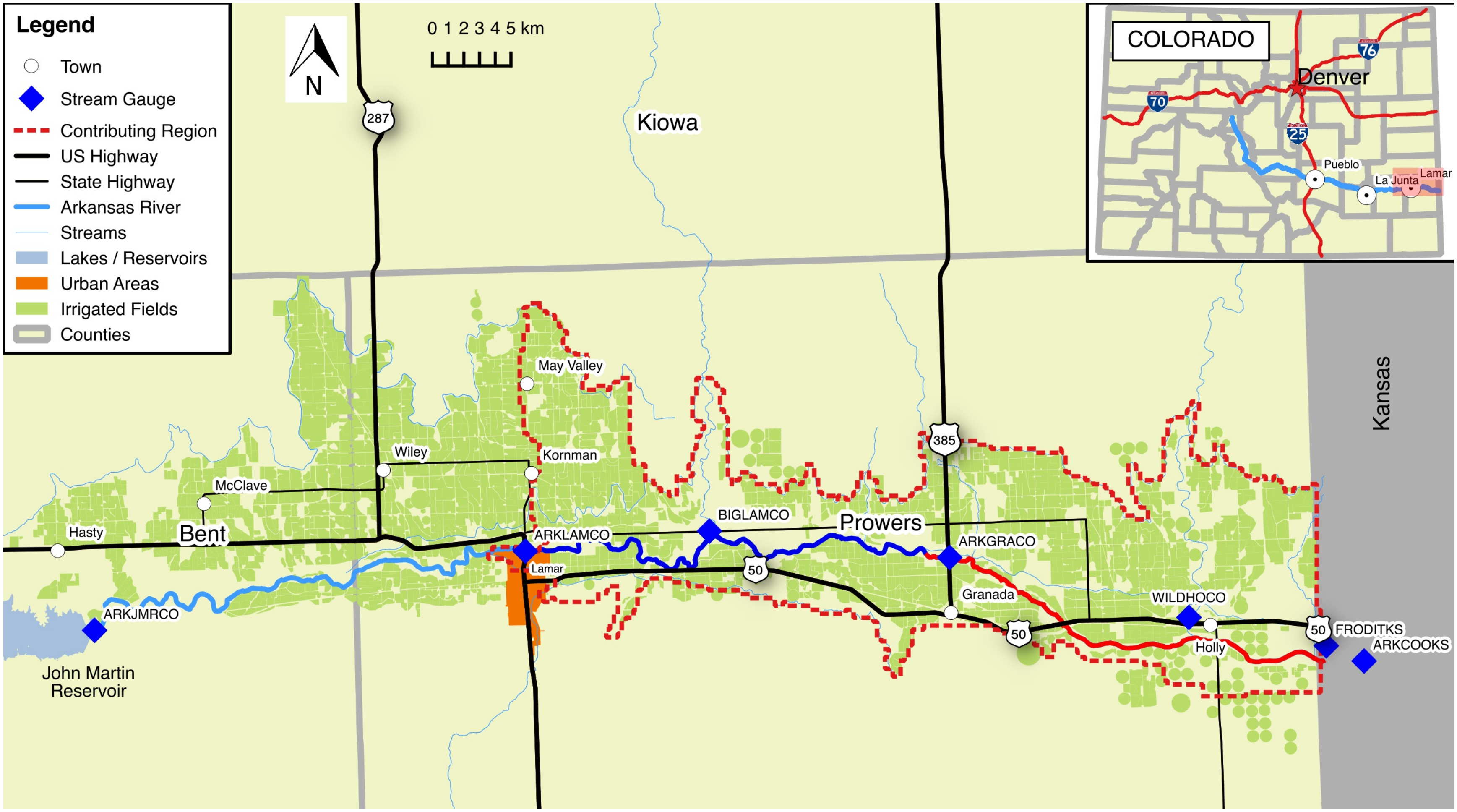

Figure 3.17. DSR River River and Tributary Stream Gauge Locations.

and reported on the CDWR web site. Note that the CDWR gauge site ARKLAMCO, which is owned by the USGS, does not have any additional data collection instruments.

Table 3.8. Summary of Stream Gauges with Notation of Additional Data Collected.

Study	Stream Gauge ID		Parameter		
Reach	CDWR	USGS	Air Temp.	Water Temp.	EC
USR	ARKCATCO			X	X
	HOLCANCO				
	RFDMANCO				
	FLSCANCO				
	RFDRETCO				
	TIMSWICO				
	FLYCANCO				
	CANSWKCO				
	ARKLAJCO		X		
	CONDITCO				
	HRC194CO				
	ARKLASCO	07124000		X	X
DSR	ARKJMRCO	07130500		X	X
	ARKLAMCO	07124000			
	BIGLAMCO				
	BUFDITCO				
	WILDHOCO				
	FRODITCKS				
	ARKCOOKS	07137500		X	X

Stream flow data were obtained as average daily flow for each stream gauge. Some average daily flow records were reported as being estimated or provisional. These data points were removed from the analysis. Average daily flow data were quality checked for unacceptable values. For each gauge, acceptable values were defined as those above zero and below the 99th percentile of all flows recorded at that gauge. Unacceptable values were removed from the data set.

All stream gauges report gauge height which is the vertical distance from the gauge site datum to the water surface (Figure 3.18). Gauge site datum is arbitrarily set, but is tied to a local survey benchmark. Flow depth is the depth from the bottom of the channel to the water's surface. While both gauge height and flow depth measure the distance to the water's surface, their datums can, and frequently do vary. The Arkansas River is a shifting bed channel and as such, the channel bottom elevation varies with time at a gauge site. The rating table, which is used to convert flow depth to flow rate, is configured such that flow depths below the channel bottom have a flow rate of zero. The table is frequently updated with data obtained from routine re-calibration of the stream gauge.

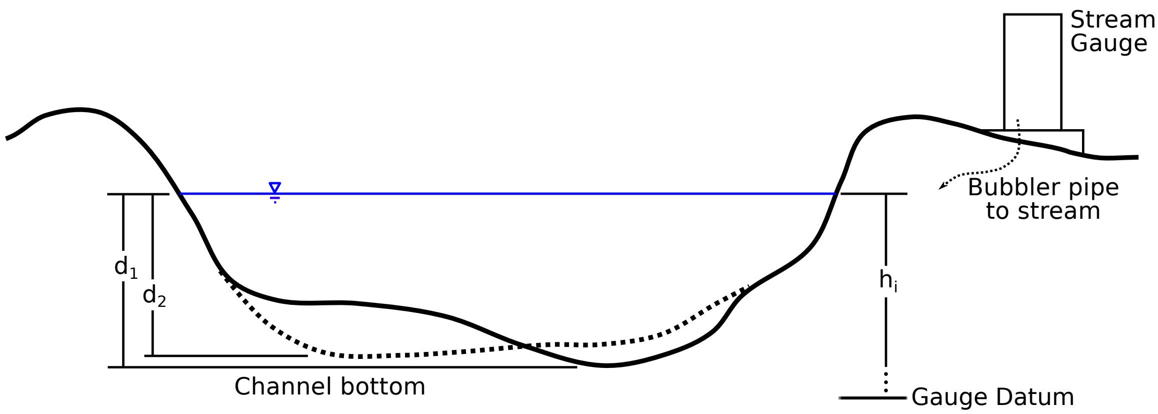

Figure 3.18. Depiction of Variable Channel Bottom and Fixed Gauge Datum. d_1 and d_2 are flow depths at different times. h_i is the stream gauge height measurement at any time.

Gauge height data is the directly measured value that is used to calculate flow rate. Flow rates are calculated from gauge height using a gauge site specific rating table produced in accordance with USGS standards and procedures (**USGS1982a**; **USGS1982b**). Gauge heights for the USGS and CDWR gauges were obtained from the respective regional offices. Historical recorded gauge heights are not reported on web sites as these data are considered to be precursors for stream flow rate calculations. Stream gauge data were provided as both average daily gauge height and as recorded gauge height. Recorded gauge height is the gauge height recorded in 15-minute increments during a calendar day. Average daily gauge height is the mean of the recorded gauge heights over a calendar day. All gauge heights were provided in units of feet above the gauge datum. Gauge height units were converted to SI units of meters for this study to simplify calculations and discussion. Gauge height data were checked for accuracy by the source agency before being released to CSU staff.

Water temperature data were obtained as average daily temperature or as minimum and maximum daily temperatures, depending on the gauge site. Average daily temperature is calculated as the mean of the minimum and maximum daily temperature. Water temperature data were provided in units of °C. Since frozen or partially-frozen river channels do not have the same gauge height to flow rate relationship as free running river channels, data corresponding to water temperatures below zero were removed from the data set.

EC data obtained from USGS and CDWR stream gauge sites were provided as average daily values for each recording gauge station. EC values recorded at the stations were compared to available EC values measured by CSU to cross-validate both data sets. Gauge station recorded EC values were quality controlled by removing the bottom and top 1% of EC values for each gauge. Changes in average daily EC between consecutive days were checked for validity. Changes greater than 33% were analyzed to determine if the EC change was valid. The average daily flow rate and time of year were taken into consideration when determining if the questionable EC values were valid. EC values that exceeded the 33% change but were accompanied by large changes in EC or during peak irrigation seasons were considered valid EC values. Values considered to be invalid were removed from the data set. EC values were provided in units of $\mu S\,cm^{-1}$.

Atmospheric data was required to determine the volume of water evaporated from the river's surface. The Colorado Agricultural Meteorological Network (CoAgMet) was chosen as the source for atmospheric data. The National Weather Service station sites in the study regions are located in populated areas or at airports and is only suitable for weather analysis. CoAgMet station sites are more numerous, are located in agricultural areas, and are suitably equipped for evaporation and transpiration (ET) analysis. An example of one of the weather stations is shown in Figure 3.19. The CoAgMet network is operated by the Colorado Climate Center at CSU and consists of 86 weather stations throughout the state. Some stations are only seasonally operational (**Andales2009**; **Csu2012**). Of the full-time sites, three are located in the USR and three are located in the DSR as shown in Figures 3.20 and 3.21, respectively. The CoAgMet weather stations in the USR are located such that they represent the upper, middle, and lower segments of the USR. The CoAgMet stations in the DSR are more tightly grouped toward the upstream end of the reach, but still are considered representative of the study reach. The weather stations are primarily located in agricultural areas to provide agricultural researchers with data used for many different research applications. The data also are available to the public through a web site. This has aided farmers in determining irrigation timing and quantity (**Andales2009**). Table 3.9 is a list of the parameters measured at the CoAgMet stations and the typical instruments used. Not all stations are identical. Instruments were replaced or upgraded by CCC staff when required with instruments that were available and equal to or better in quality than the instrument being replaced.

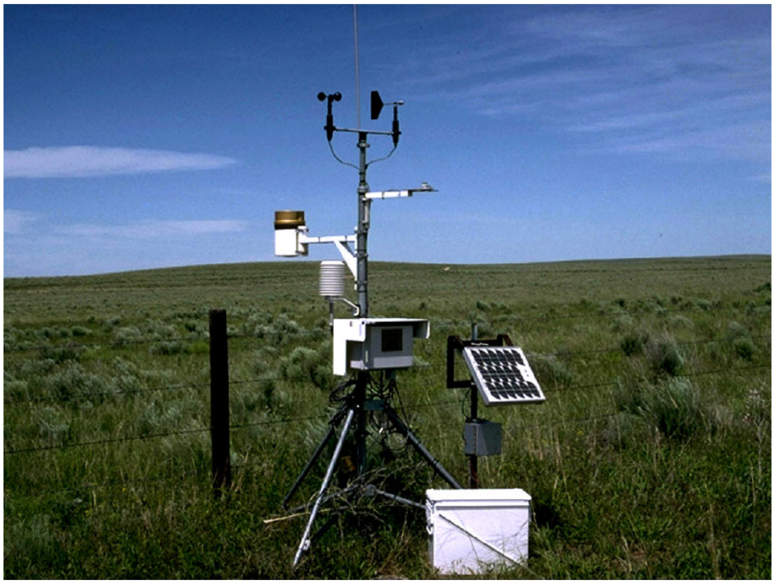

Figure 3.19. Typical CoAgMet Weather Station.

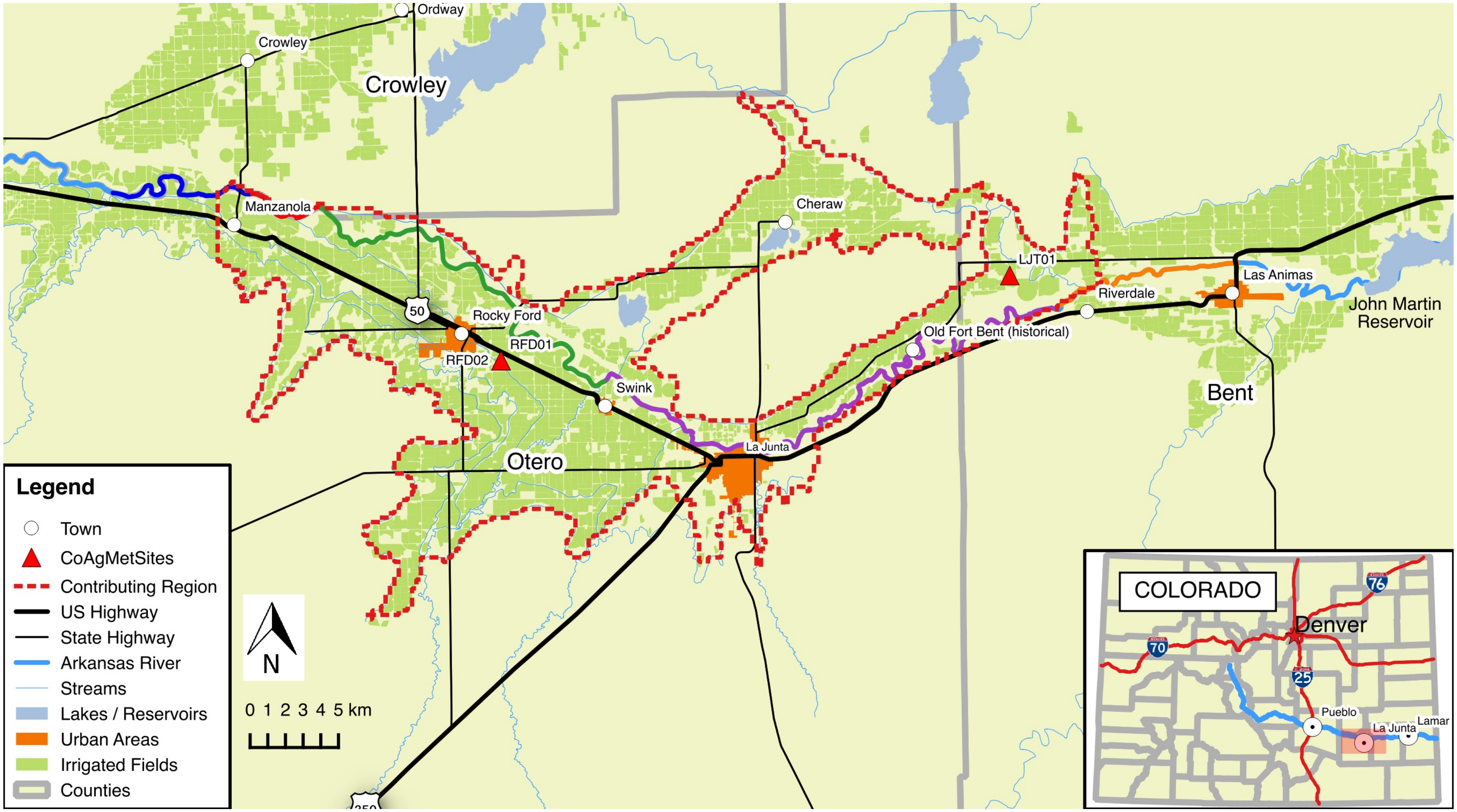

Figure 3.20. USR CoAgMet Weather Station Locations.

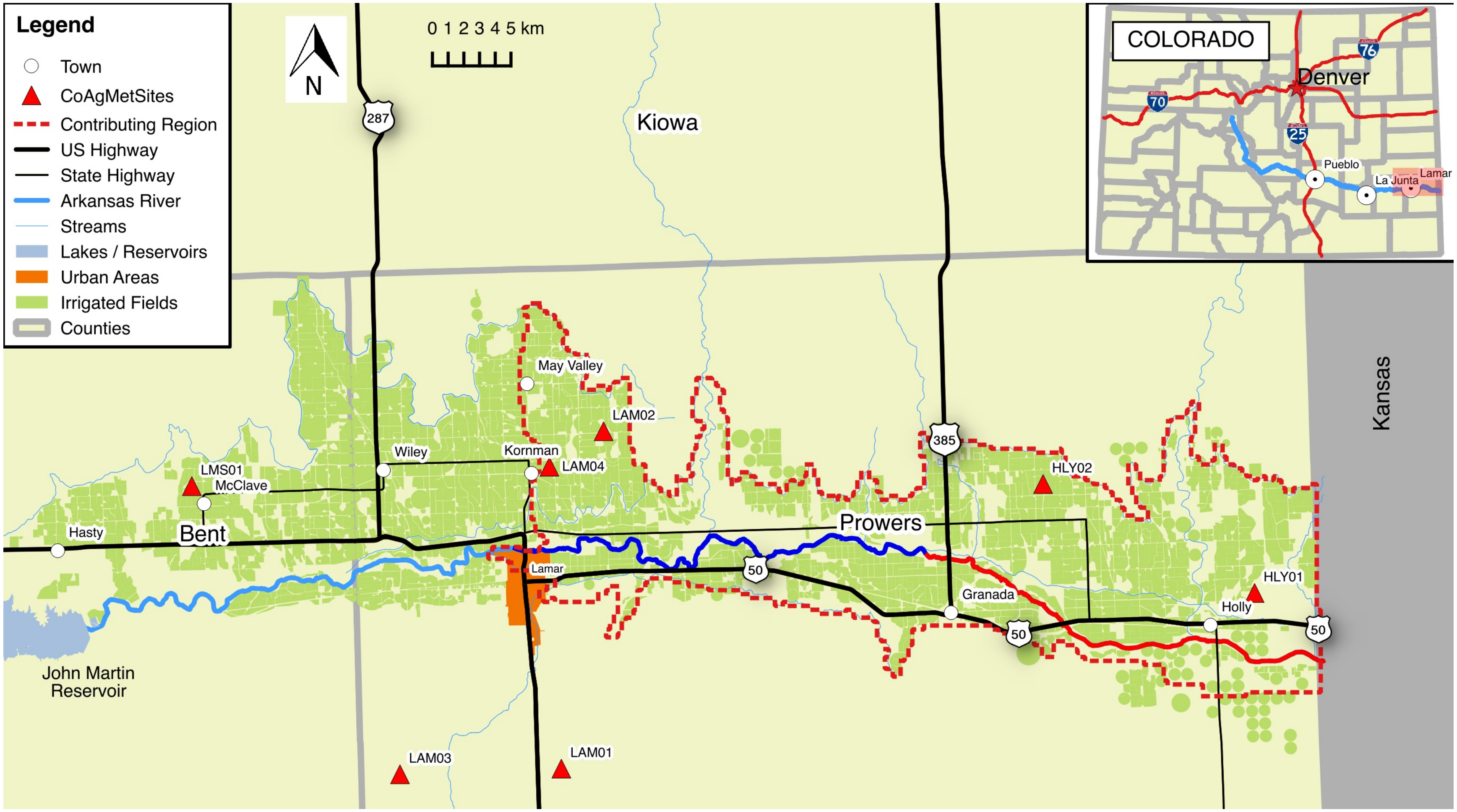

Figure 3.21. DSR CoAgMet Weather Station Locations.

Table 3.9. Typical Instrumentation at CoAgMet Weather Stations.

Measured Parameter	Typical Instrument
Temperature & Relative Humidity	Vaisala HMP45C Probe
Wind	R.M. Young Wind Sentry
Solar Radiation	Licor LI-200X Pyranometer
Precipitation	TE525 tipping bucket raingauge
Soil Temperature	CSI Model 107 Soil Temp Probe (thermistor)
Data Loggers	Campbell Scientific CR10, CR10X, and CR1000

Table 3.10 lists the weather stations in the LARV that were used in this study. This table lists the station name and location, the state of irrigation of the land surrounding the site, the date of first record, and a comparative estimate of the site estimated ET_{ref} to the actual ET_{ref}. The irrigation state of the land surrounding the site is used to determine the comparative estimate of the site estimated ET_{ref} to the actual ET_{ref}. If the monitoring station is on irrigated land then the ET_{ref} values calculated based on site data are expected to be at or near the actual value of ET_{ref} for the site. If the station is on dry, or non-irrigated land, then calculated ET_{ref} values tend to over estimate the actual ET_{ref}.

CoAgMet provides both raw weather data from all weather stations and daily ET_{ref} values calculated for select stations. Daily ET_{ref} values were obtained from the sites in the LARV. The American Society of Civil Engineers (ASCE) Environmental and Water Resources Institute (EWRI) standardized tall crop evapotranspiration reference Penman-Monteith equation was used by the Colorado Climate Center to calculate ET_{ref}. Values are obtained in units of $\mathrm{mm\,d^{-1}}$.

The average daily ET_{ref} for a region surounding a study reach was calculated as the mean of the stations reporting ET_{ref} for a given day. If a station or group of stations did not have data for a particular day in the study time frame, then then those stations were not included in the calculation. An assumption was made that the ET_{ref} over the Arkansas

Table 3.10. CoAgMet Weather Stations used for analysis in the LARV.

Study Reach	Station ID	Station Name	Station Location	Irrigation	Date of First Record	Comparative Est. of Site ET
USR	FWL01	Fowler	Fowler Golf Course	Full	17 Mar 2005	–
	LJT01	LaJunta	11 mi NE of LaJunta	Full	17 Mar 2005	Under
	RFD01	RockyFord	CSU Experiment Station, Rocky Ford	Full	6 Apr 1992	–
DSR	HLY01	Holly	5 mi NW of Holly	Part	27 Sep 2001	Over
	HLY02	Holly #2	8.5 mi NW of Holly	Full	21 May 2005	–
	LAM04	Lamar #4	4.5 mi NNE of Lamar	Full	11 May 2005	–

River within a study reach could be approximated as the mean of the reported values within the surrounding region.

The minimum daily relative humidity (RH_{min}) and wind speed at 2 m above ground surface (u_2) data were obtained from the same CoAgMet stations as the precipitation and ET_{ref} data. RH_{min} values were reported as a fraction and values less than zero were removed from the data set. Wind speed values were reported as wind run, which is the total distance the air traveled during the calendar day and is reported in units of $\mathrm{km\,d^{-1}}$. A small number of the wind run values in the obtained data set were less than zero and were removed. Historical average wind run values were not available to provide a method to sanitize the wind run upper bound values. Wind run values were converted to average daily wind speed in units of $\mathrm{m\,s^{-1}}$.

Precipitation data were collected from the same network of monitoring stations used to generate average daily ET_{ref} as daily values in units of $\mathrm{mm\,d^{-1}}$. Data was not sanitized before publication to the CoAgMet web site. A small number of total daily precipitation values in the obtained data set were less than zero or exceeded reasonable maximum values. Daily total precipitation values less than zero or greater than 1.5 times the highest average precipitation reported by the National Weather Service were excluded. As with the ET_{ref} data, the mean precipitation value over the surrounding region of a study reach for any given day only included those stations reporting data. Any additional data collected from the CoAgMet system was treated in a similar manner.

CHAPTER 4

Evaluation of NPS Return Flow to the River Using a Water Balance Model

4.1. Water Balance Model Applied to the LARV

Water Balance Model Equation.

The purpose of the water balance model is to determine the volume of unaccounted for water in each reach. We begin with a basic water balance model as describe in most hydrology texts — (Wanielista, Kersten, Eaglin, et al. 1997).

$$\text{change in storage} = \text{inputs - outputs}$$

Adding the variables, both known and unknown, present in the LARV we have the following equation:

$$\frac{\Delta S}{\Delta t} = Q_{in,US} + \sum Q_{in} + P + R + B - Q_{out,DS} - \sum Q_{out} - E - T - F \tag{3}$$

Where:

$\frac{\Delta S}{\Delta t} =$ Stored volume change between time steps.

$Q_{in,US} =$ Flow in the river entering the study reach at the upstream end.

$\sum Q_{in} =$ Flow gained by the river from tributaries and other gauged sources.

$P =$ Volume of water gained to the river due to precipitation falling directly on the river's surface.

$R =$ Volume of water gained to the river due to precipitation runoff from adjacent land.

$B =$ Volume of water gained to the river due to subsurface flow.

$Q_{out,DS} =$ Flow in the river leaving the study reach at the downstream end.

$\sum Q_{out}$ Flow lost from the river to canals and other gauged sinks.

$E =$ Volume of water lost from the river due to direct evaporation from the water's surface.

$T =$ Volume of water lost from the river due to plant transpiration.

$F =$ Volume of water lost from the river due to infiltration into the subsurface flow.

If we combine the terms that are unknown or unmeasured, we arrive at the following equation:

$$\frac{\Delta S}{\Delta t} = Q_{in,US} + \sum Q_{in} + P - Q_{out,DS} - \sum Q_{out} - E + Q_{NPS} \tag{4}$$

Where:

$Q_{UNPS}=$ The sum of gains from non-point sources and losses to non-point sinks ($Q_{NPS} = R + B - T - F + Q_{U,in} - Q_{U,out}$).

There is no reasonable method for differentiating the components of Q_{UNPS}, therefore the abbreviation NPS in this thesis refers to both non-point sources and non-point sinks. Q_{UNPS}includes the non-point source gains from groundwater sources(B), non-point source losses to groundwater sinks F), transpiration losses from plants in the river channel (T), and gains from precipitation runoff from adjacent land (R). Additionally, this term includes ungauged flows leaving and entering the river. Ungauged gains to the river ($Q_{U,in}$) are suspected to be primarily in the form of irrigation drainage from adjacent farmland. Other sources could be due to errors in underestimating flows entering the river or overestimating flows leaving the river. Ungauged losses from the river ($Q_{U,out}$) are suspected to be primarily in the form of minor or unauthorized withdrawals from the river channel. Of the ungauged flows, irrigation drainage from adjacent farmlands is assumed to be the largest contributor.

The two groundwater components of $Q_{UNPS}$are suspected of being the largest components of Q_{UNPS}. Water transfer between the aquifer and river happens continually whereas $Q_{U,in}$, $Q_{U,out}$, R, and T are not continuous. $Q_{U,in}$ and $Q_{U,out}$ only occur periodically when individuals actively withdraw from the river or allow irrigation runoff to return to the river. R only occurs during rain events. Within the LARV, most rainwater is captured in irrigation canals. Only precipitation falling in the riparian zone is likely to reach the river. T only occurs during growing season. This value is also only considering the transpiration happening within the river channel and does not include the riparian zone. Any losses due to transpiration in the riparian zone are first considered river losses to the aquifer (F).

Re-arranging equation (4) to solve for the unknown values produces equation 5. Due to the nearly identical method of calculating flow (Q) and it's associated error and uncertainty, these terms were associated with each other. Likewise, the precipitation (P) and evaporation (E) terms were associated with each other.

$$Q_{UNPS} = \left(Q_{out,DS} + \sum Q_{out} - Q_{in,US} - \sum Q_{in}\right) - \frac{\Delta S}{\Delta t} - (P + E) \tag{5}$$

A time step of one day was established for all models calculated in this thesis. Most of the data from agencies is readily available in average daily format. While most of the data could also be obtained in hourly or quarter-hourly format, it was assumed that the additional information would not improve model accuracy.

4.2. Stochastic and Deterministic Models

Deterministic and stochastic models are used in both the unaccounted for water and mass balance models. Deterministic models are fully determined by the input parameters or variables. Randomness of any kind is not included. Stochastic models extend deterministic models by including one or more random parameters. Given the same input parameter values, a stochastic model will produce different results with each iteration.

There are many recognized methods for solving stochastic models. Solutions to these models are not definite and the term ”solve” must be taken loosely. Any individual solution from a stochastic model is one of a potentially infinite number of possible solutions. The Monte Carlo (MC) simulation technique was used to obtain solutions for all stochastic models in this thesis. The MC technique is conceptually simple. The stochastic model is repetitively solved in a series of iterations. The combined solutions from all iterations are used to define the solution statistics of the model.

The number of iterations performed is determined in a number of ways. One way is to calculate a set of identifier statistic(s) after each run. Identifier statistic(s) are those that the modeler has determined to be of value in determining when to terminate the model. Usually, these statistics are monitored to identify when the change in the statistic has reached a predetermined threshold. An alternate method of determining the number of iterations to perform is more fixed. The model is run for a estimated number of iterations. A set of results for each iteration is saved. After all iterations are calculated the identifier statistic(s) are calculated for each iteration. The modeler then determines the number of iterations based on the results. The modeler must determine the best method based on a number of factors to include software and hardware limitations and the limits of the modeler's programming skills.

It was determined that for the sake of simplicity, all of the models calculated in this thesis would use the same number of iterations. The USR mass balance model is the most complex model as it has the largest number of input variables and uncertainty terms. The identifier statistics used were the mean, variance, and skewness, which are the first, second, and third moments of the probability density. These were calculated for each iteration. The threshold between the observed iteration and the previous iteration was fixed at 0.1%. The identifier statistics reached the threshold in the following order: mean, variance, and skewness. Skewness reached its break point shortly before the 500th iteration. A judgment call was made to increase the factor of safety. Therefore, the number of stochastic model iterations was fixed at 5,000.

4.3. Error and Uncertainty.

Any problem that measures variable natural processes must account for parameter and model uncertainties (Vicens, Rodríguez-Iturbe, and Schaake 1975). Parameter uncertainty is derived from measurement error, spatial variability, and temporal variability (Herschy 2002). Measurement error is the difference between the true and measured values. Most of this error type is due to instrument measurement inaccuracies due to either error inherent in the instrument or from errors in calibration or measurement. Measurement errors inherent to the instrument are uncorrectable and cannot be accounted for within the model. Errors due to calibration or measurement deviations are only correctable at the time of measurement or calibration and cannot be accounted for within the model.

Spatial variability is the difference in the true value at different points when measured at the same time. Data collected at a single given point in space may not be representative of the area it is assumed to represent due to spatial variability. This can manifest itself even with very small distances between measurements. Temporal variability is the difference in the true value at the same point, but at different times. Data collected at a one time may not be representative of the time frame it is assumed to represent due to temporal variability (Gates and Al-Zahrani 1996). Again, this can be manifested even over small time differences. Due to instrument error, the spatiotemporal variability of the measured object, and the inability to know the true value of the measurement, reported parameter values should be treated as random variables (C. T. Haan 1989; Charles Thomas Haan 2002).

Almost all of the data was obtained from outside agencies and was not collected by the research team. These agencies have data uncertainty ranges that account for all parameter uncertainties. These uncertainties are expressed in accordance with the ISO Guide to Expression of Uncertainty in Measurement (GUM) (ISO 2008). While the GUM classifies uncertainty as either "Type A" or "Type B", the all of the data included in this thesis has uncertainty evaluations described as "Type B". Type B evaluations usually use standard deviations and assumed probability distributions obtained from scientific judgment, available information, and possible variability of a measurement.

For most of the data used in this thesis, we are not the data originators. The data originators have provided uncertainty ranges which include instrument measurement random error and uncertainties due to temporal variations of the measured location. The root mean square method is used to estimate the uncertainty related to measurement of water quantity and water quality values (Harmel and Smith 2007; ISO 2008). Harmel and Smith (2007) describe this measurement uncertainty as the probably error range, and quantify upper and lower uncertainty boundaries for measured data points as the following when attempting to specify an expected range of expected values.

$$\sigma^2 = \left(\frac{O_i - UO_i(l)}{3.9}\right)^2 \qquad or \qquad \sigma^2 = \left(\frac{UO_i(u) - O_i}{3.9}\right)^2 \tag{6}$$

Where:

$\sigma^2 =$ variance about measured data value O_i.

$O_i =$ measured value.

$UO_i =$ upper (u) and lower (l) uncertainty boundaries.

$3.9 =$ number of standard deviations accounting for $> 99.99\%$ of a normal probability distribution

The data collected for this thesis is assumed to represent the mean of a normal distribution of possible values. The upper and lower bounds of the distributions are given as either a percent or value deviation from the mean. Equation 6 is re-written from the definition found in Harmel and Smith (2007) to that found in equation 7.

$$\sigma^2 = \left(\frac{\mu - (\mu - \mu p)}{3.9}\right)^2 \qquad or \qquad \sigma^2 = \left(\frac{(\mu + \mu p) - \mu}{3.9}\right)^2 \tag{7}$$

Where:

$\mu =$ the reported value (assumed to be the mean).

$p =$ the reported percent deviation from μ.

Both of these equations in 7 simplify to equation 8. The standard deviation is shown as the calculated result due to the requirements of the calculating software.

$$\sigma = \frac{\mu p}{3.9} \tag{8}$$

When the upper and lower bounds are defined as a value deviation from the reported value, then equation 6 becomes:

$$\sigma^2 = \left(\frac{\mu - (\mu - v)}{3.9}\right)^2 \qquad or \qquad \sigma^2 = \left(\frac{(\mu + v) - \mu}{3.9}\right)^2 \tag{9}$$

Where:

$v =$ the reported value deviation from μ.

In this case, both equations in 9 simplify to:

$$\sigma = \frac{v}{3.9} \tag{10}$$

The difference between a model's calculated or estimated value and the reported value is called a residual. The distribution of residuals is the model uncertainty. These distributions are uni-variate and do not have predefined shapes. There are a variety of statistical and graphical tools available to analyze unknown residual distributions to determine a best fit parametric distribution. The two graphical tools used in this thesis are the histogram and the kernel density plot.

Non-parametric distribution models are used as an aid for analyzing uni-variate data sets. Specifically, kernel density estimates (KDE) are used in conjunction with histograms to assist in visual analysis of the data. Figure 4.1 is an example of a random sample of one of the input data sets used in this thesis. The curve is the KDE. The short vertical lines between the histogram and the x-axis, called a rug, depict the data values. This figure adequately displays the resulting differences between histograms and KDE. KDEs can more accurately depict data groupings that are lost in histogram bins. The histogram leads us to believe that the data has a strong tendency to be near zero, wile the KDE shows that the majority of the data is between 0-20. Histograms can more accurately depict extremes or cut-off values. In the figure, there are no values less than zero. The histogram clearly shows this while the KDE shows that there are values less than zero. Both histograms and KDE are used throughout this thesis to assist in the description of distributions. A rug is also presented with the histogram whenever the quantity of data allows for adequate data presentation. A rug is not included when the data set is too large to allow for discreet identification of data values.

Determining which parametric distribution best fits the uni-variate residual distribution requires the use of both the graphical and statistical tools. For each residual distribution, probable parametric distributions types were chosen for testing against the residual distribution. For each of these parametric distribution types, a best fit was generated using the maximum likely-hood estimator (MLE) method. These MLE results were then analyzed using Kolmogorov-Smirnov (K-S), Cramer-von Mises (CvM), and Anderson-Darling (A-D) goodness-of-fit tests to determine which distribution type best fit the uni-variate residual distribution. All three tests are non-parametric tests of continious uni-variate probability distributions. The K-S and CvM tests calculate the difference between the empirical cumulative density function (ECDF) of the test data and the cumulative density function (CDF) of the tested reference distribution. The K-S and CvM tests use different algorithms to perform

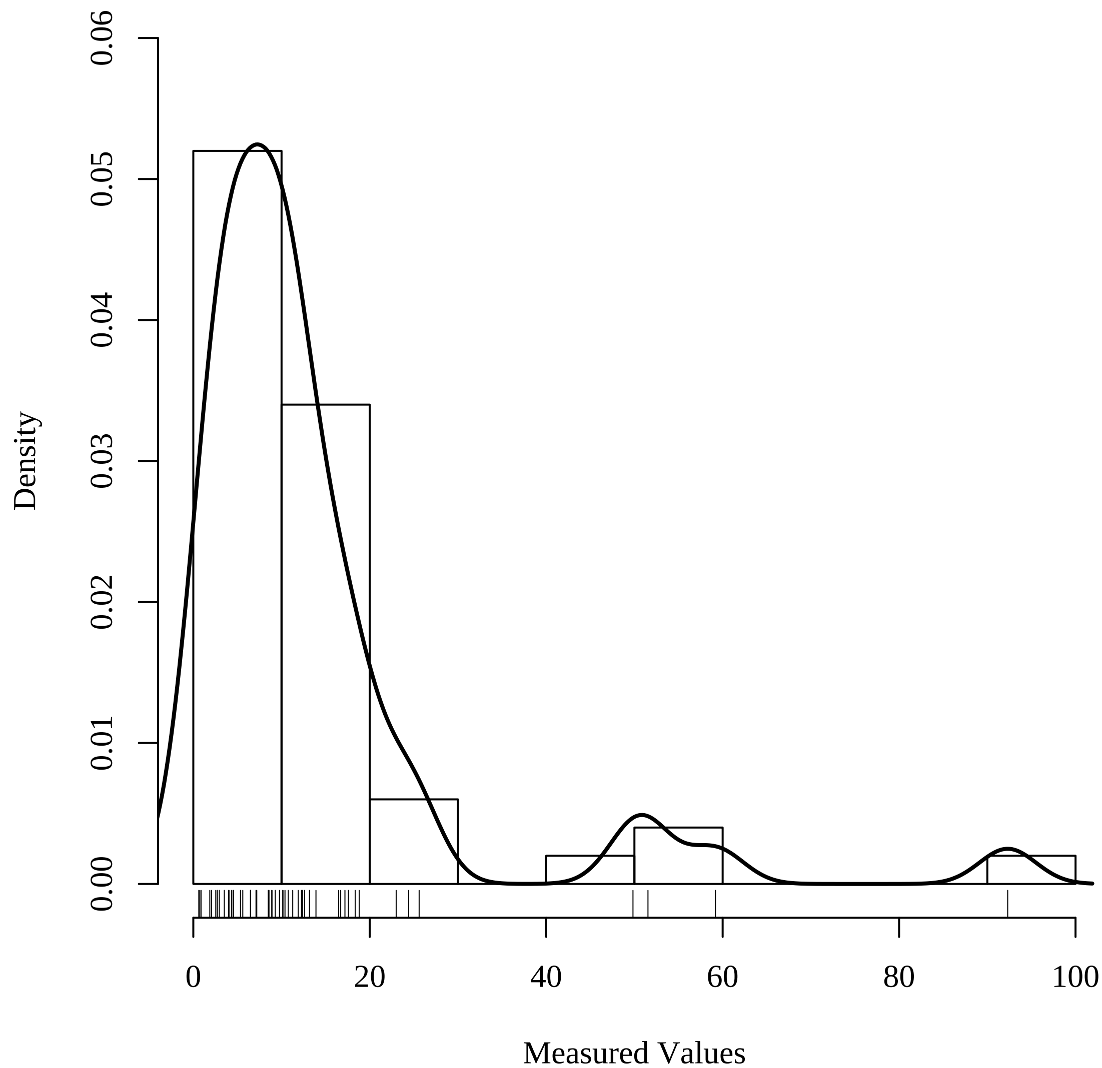

Figure 4.1. Example kernel density estimate. The data is a random sample of an input variable used in this thesis. The curve depicts the kernel density estimate. The short vertical lines between the histogram and the x-axis, called a rug, depict the data values.

the calculation. Each of the goodness-of-fit tests has their own strength and weaknesses and as such, graphical tools are used to confirm or refute the statistical test results (D'Agostino and Stephens 1986; Delignette-Muller and Dutang 2014; Venables and Ripley 2002).

4.4. River Storage Change

River reach estimated stored water volume changes ($\frac{\Delta S}{\Delta t}$) from equation 3 are the sum of the river segment stored water volume changes for each reach (Equation 11). The storage change for each segment is calculated independent of adjacent segments.

$$\frac{\Delta S}{\Delta t} = \sum \frac{\Delta S_i}{\Delta t} \tag{11}$$

Where:

$\Delta S =$ Water storage change in the river reach.

$\Delta S_i =$ Water storage change in river segment i.

$\Delta t =$ Model time step = 1 day.

River reach volume changes are calculated between two consecutive time steps. Reach volume changes are calculated as the sum of the volume changes within the segments that compose the reach. River segment volume change between time steps is calculated as shown in equation 12.

$$\frac{\Delta S_i}{\Delta t} = L_i \cdot \frac{\Delta A_i}{\Delta t} \tag{12}$$

Where:

$\frac{\Delta S_i}{\Delta t}$ = Segment storage change.

L_i = Segment length.

$\frac{\Delta A_i}{\Delta t}$ = Segment cross-section area change.

Figure 4.2 shows the difference between a simplified example of a natural channel and the modeled channel. Although the river is variable in width and depth along its entire lengths, it is modeled as a trapezoidal prism with a constant length and with a cross-section that does not vary with respect to location. It was reasoned that this simplistic model would best approximate the average channel shape along the entire reach. The channel water surface elevation is assumed to be constant through each segment. This assumption is not true in nature, but we are not concerned with the water surface elevation, but with the flow depth. We are assuming that the flow depth remains relatively constant through a river segment. This assumption assumes that all gains and losses to the river are accounted for either through flow gains and losses, evaporation, precipitation, or unaccounted for gains and losses as shown in equation

eq Ref

. eq ref

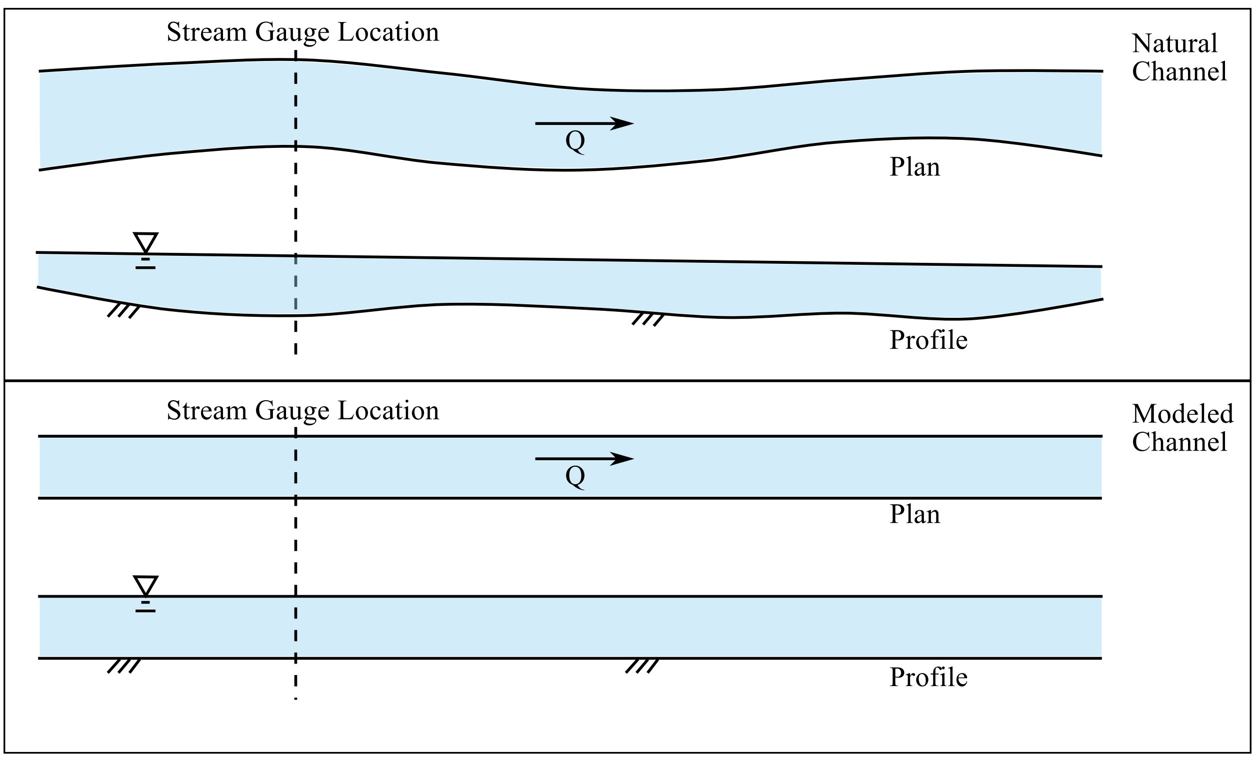

Figure 4.2. River Segment Model.

Segment lengths, as reported in Table 4.2, are sufficiently short such that any surges due to irrigation canal gates changes, precipitation events, or other events pass through the segment in less than a day. The total travel time in the USR is 2-3 days and 1-2 days in the DSR based on USGS reported average stream velocity measurements taken in conjunction with stream gauge calibrations. River segment length (L_i) was measured to the nearest 0.1 km using publicly available satellite imagery, USGS hydrography data, and geographical information system (GIS) software. River segment length was calculated as the length of the thalweg between the segment endpoints. When the USGS thalweg did not follow along the river channel as shown in the satellite imagery, a new thalweg was drawn. Rough validation of these measurements was performed in the field by comparing the GIS calculated length of adjacent roadways to the actual driven distance as reported by a vehicle odometer. River lengths are assumed to be constant throughout the study time frame. Individual and combined variations in the channel path along a river segment were assumed to be negligible.

Table 4.2. River Segment Lengths.

Study Reach	River Segment	Segment Length km	Segment Length mi
USR	A	12.5	7.8
	B	3.9	2.4
	C	30.7	19.1
	D	37.8	23.5
	E	14.3	8.9
DSR	F	37.6	23.4
	G	24.9	15.5

River segment cross-sectional area change $\left(\frac{\Delta A_i}{\Delta t}\right)$ calculation is based on the trapezoidal area that is composed by the difference between the cross-sectional area at two different flow depths as depicted in Figures 4.3 4.4 and in equation 13. Figure 4.3 shows a simplified river cross section at a stream gauge location. As previously discussed, stream gauges do not hold the channel bottom as their datum. They have an arbitrarily fixed datum that does not move unless determined by the gauge owner.

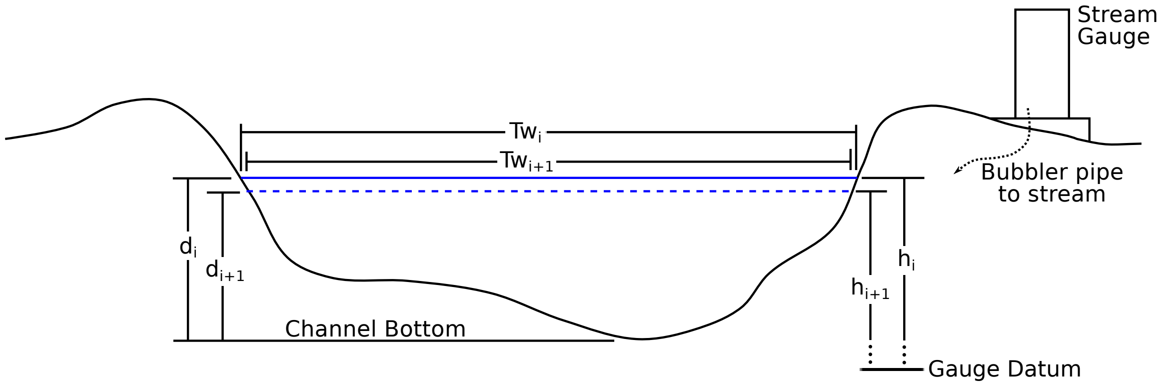

Figure 4.3. Average river segment cross-section area change.

change d to y

change d to y - font

$$\Delta A = \overline{Tw} \cdot \Delta y$$

$$\Delta A = \frac{Tw_t + Tw_{t-1}}{2} \cdot (y_{t-1} - y_t) \tag{13}$$

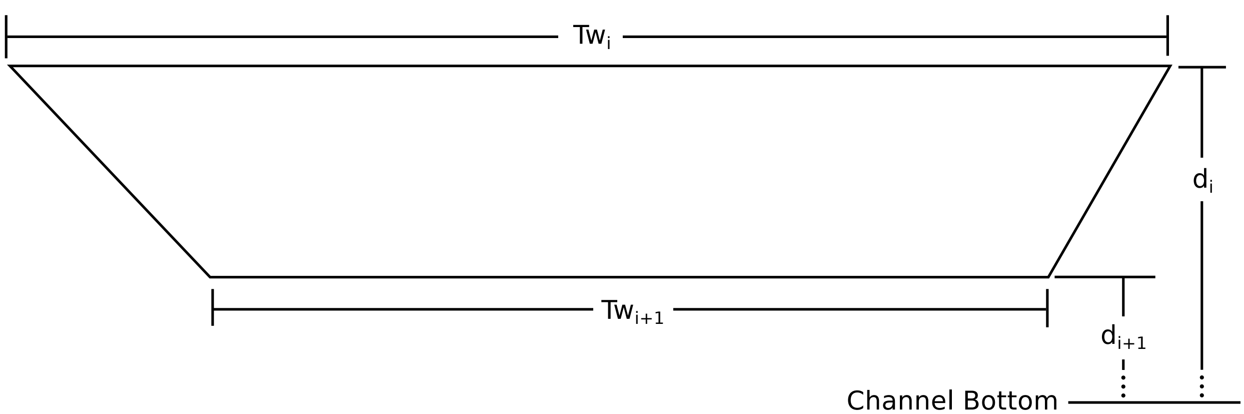

Figure 4.4. River cross-section area change diagram.

Where:

subscript $_t$ = Current time step.

subscript $_{t-1}$ = Previous time step.

ΔA = Cross-section area change.

$\overline{Tw}$ = Average river top width.

Δy = Change in flow depth from the previous time step.

Tw = River top width.

y = River flow depth.

Flow depth values as reported by the USGS and CDWR are measured values with an associated probability range as calculated in equation 8. The uncertainties are applied as shown in equation 14. A correction factor (C_i) is applied to each reported gauge depth to correct for the difference between the gauge datum and the channel bottom as measured during the channel cross-section survey. Two separate uncertainties are applied. ε_{h1} is the uncertainty distribution as described by the gauge owner. This uncertainty is reported by the USGS and CDWR as a accuracy rating of excellent, good, fair, or poor. Each of these designations corresponds to a uncertainty distribution as published by the USGS and show in Table 4.3 which is extracted from one of the USGS annual water reports . These uncertainty designations and their associated distributions are valid only at the respective gauge site. The second uncertainty term, ε_{h2}, is the result of personal observation of the river channel along its entire length. This term describes the variability in flow depth. It was observed that the channel depth did not vary greatly along most of its length. There were particular areas where there were deeper pools, but these areas were noted to be more prone to ponding

cite USGS water reports

during low flow. It is assumed that the average effective flow depth only varies within a normal distribution with limits of $\pm 0.076\,\mathrm{m}$ ($\pm 0.25\,\mathrm{ft}$).

$$y_{i,t} = h_{i,t} + C_i + \varepsilon_{h1} + \varepsilon_{h2} \tag{14}$$

Where:

$y_{i,t} =$ Section i modeled flow depth at time t.

$h_{i,t} =$ Section i reported river gauge height at time t.

C_i Section i river gauge height to flow depth correction term

$\varepsilon_{h1} =$ Reported river gauge data uncertainty.

$\varepsilon_{h2} =$ Estimated flow depth uncertainty.

Table 4.3. USGS Measured Field Parameter Accuracy Rating Table. This table was taken from the USGS annual water data report.

Measured field parameter	**Ratings of accuracy (Based on combined fouling and calibration drift corrections applied to the record)**			
	Excellent	**Good**	**Fair**	**Poor**
Water temperature	≤ ± 0.2 °C	> ± 0.2 - 0.5 °C	> ± 0.5 - 0.8 °C	> ± 0.8 °C
Specific conductance	≤ ± 3%	> ± 3 - 10%	> ± 10 - 15%	> ± 15%
Dissolved oxygen	≤ ± 0.3 mg/L or ≤ ± 5%, whichever is greater	> ± 0.3 - 0.5 mg/L or > ± 5 - 10%, whichever is greater	> ± 0.5 - 0.8 mg/L or > ± 10 - 15%, whichever is greater	> ± 0.8 mg/L or > ± 15%, whichever is greater
pH	≤ ± 0.2 units	> ± 0.2 - 0.5 units	> ± 0.5 - 0.8 units	> ± 0.8 units
Turbidity	≤ ± 0.5 turbidity units or ≤ ± 5%, whichever is greater	> ± 0.5 - 1.0 turbidity units or > ± 5 - 10%, whichever is greater	> ± 1.0 - 1.5 turbidity units or > ± 10 - 15%, whichever is greater	> ± 1.5 turbidity units or > ± 15%, whichever is greater

River segment B in the USR does not have a flow gauge within its boundaries and therefore has no reported flow depths. This segment has an additional irrigation diversion check structure within its boundaries, thereby sub-dividing segment B into two sub-segments, each with its own ungauged flow depth. Due to segment B being the shortest, composing only 3.9% of the USR's total length, and the additional variability of the possible flow depth, the average daily flow depth within segment B is taken as the mean of the reported flow depths in segment A and C. Top width and volume change calculation follows the previously described methodology.

References

D'Agostino, Ralph B. and Michael A. Stephens, eds. (1986). *Goodness-of-fit-techniques (Statistics: a Series of Textbooks and Monographs, Vol. 68)*. 1st ed. Dekker. ISBN: 9780824774875.

Delignette-Muller, Marie Laure and Christophe Dutang (2014). "fitdistrplus: An R Package for Fitting Distributions." In:

Gates, Timmothy K. and Muhammad A. Al-Zahrani (1996). "Spatiotemporal Stochastic Open-Channel Flow. I: Model And Its Parameter Data." In: *Journal of Hydraulic Engineering* 122.11, pp. 641–651.

Haan, C. T. (1989). "Parametric Uncertainty in Hydrologic Modeling." In: *Transactions of the ASAE* 32.1, pp. 0137–0146.

Haan, Charles Thomas (2002). "Statistical methods in hydrology." In:

Harmel, R Daren and Patricia K Smith (2007). "Consideration of measurement uncertainty in the evaluation of goodness-of-fit in hydrologic and water quality modeling." In: *Journal of Hydrology* 337.3, pp. 326–336.

Herschy, RW (2002). "The uncertainty in a current meter measurement." In: *Flow Measurement and Instrumentation* 13.5, pp. 281–284.

ISO (2008). "Guide to the Expression of Uncertainty in Measurement, (1995), with Supplement 1, Evaluation of measurement data, JCGM 101: 2008." In: *Organization for Standardization, Geneva, Switzerland.*

Venables, William N and Brian D Ripley (2002). *Modern applied statistics with S.* Springer Science & Business Media.

Vicens, Guillermo J., Ignacio Rodríguez-Iturbe, and John C Schaake (1975). "Bayesian generation of synthetic streamflows." In: *Water Resources Research* 11.6, pp. 827–838.

Wanielista, Martin, Robert Kersten, Ron Eaglin, et al. (1997). *Hydrology: Water quantity and quality control.* John Wiley and Sons.